

On Oscillatory Fast-Time Instability of Diffusion Flames

J. S. Kim¹ and V. V. Gubernov²

¹Air Resources Research Center
Korea Institute of Science and Technology, Seoul, 136-791, KOREA

² International Laser Center
M.V.Lomonosov Moscow State University, Moscow 119899, RUSSIA

Abstract

Fast-time instability is investigated for diffusion flames with Lewis numbers greater than unity by employing the numerical technique called the Evans function method. Since the time and length scales are those of the inner reactive-diffusive layer, the problem is equivalent to the instability problem for the Liñán's diffusion flame regime. The instability is primarily oscillatory, as seen from complex solution branches and can emerge prior to reaching the upper turning point of the S-curve, known as the Liñán's extinction condition. Depending on the Lewis number, the instability characteristics is found to be somewhat different. Below the critical Lewis number, L_c , the instability possesses primarily a pulsating nature in that the two real solution branches, existing for small wave numbers, merges at a finite wave number, at which a pair of complex conjugate solution branches bifurcate. For Lewis numbers greater than L_c , the solution branch for small reactant leakage is found to be purely complex with the maximum growth rate found at a finite wave number, thereby exhibiting a traveling nature. As the reactant leakage parameter is further increased, the instability characteristics turns into a pulsating type, similar to that for $L < L_c$.

1 Introduction

The fast time instability is a class of intrinsic combustion instabilities with the length and time scales of the inner reactive-diffusive layer instead of the conventional flame scales based on the outer convective-diffusive layer. In the context of AEA (Activation-Energy Asymptotics), where the Zel'dovich number β , a ratio of the activation energy to the thermal energy, serves as the large expansion parameter, the inner reactive-diffusive layer is thinner than the outer convective-diffusive layer by $O(\beta)$. Moreover, the corresponding time scale is $O(\beta^2)$ shorter and so arrives the name, fast-time instability [1].

The issue of fast-time instability was first raised by Peters [2], who was concerned with instability of the inner zone structure of the Liñán's premixed-flame regime [3]. Since then, the fast-time instability analysis was extended to diffusion flames by Buckmaster et al. [1], who coined the terminology of the "fast-time instability," and to effects of three-dimensional reaction zone [4], of Lewis numbers greater than unity [5], of Lewis numbers less than unity [6], of the damping effect coming from the outer layer [7]. However, none of these papers are concerned with the full spectral characteristics of the fast-time instability. Spectral characteristics of fast-time instability was first considered by Kim, Williams and Ronney [8] when they analyzed diffusional-thermal instability of diffusion flames.

In light of the previous works on the fast-time instabilities, the fast-time instability is seen to be physically relevant for the conditions sufficiently far from the bifurcation condition. Moreover, the fast-time instability is the most succinct form of intrinsic flame instability formulation because it is a purely unsteady reactive-diffusive problem. Therefore, the problem would be

a useful model to study the generic nature of the Turing instabilities [9] encountered in combustion systems. Recently, Kim and Gubernov [10] carried out an asymptotic as well as numerical analysis of the fast-time instability of the Liñán's diffusion-flame regime in order to provide a complete picture of the fast-time instability for diffusion flames with Lewis numbers less than unity. This paper is an extension of their previous work to Lewis numbers greater than unity, for which oscillatory instabilities are anticipated. Since the nature of instability is oscillatory, the eigenvalue and the corresponding eigenfunction are complex. Particularly toward the boundaries extending to $\pm\infty$, sinusoidally oscillating eigenfunctions with exponentially decaying amplitudes could pose a numerical difficulty when the fast-time instability is solved by conventional numerical methods such as the shooting method. In order to avoid such difficulties, the Evans function method [11], which has been successfully demonstrated by Kim and Gubernov in solving for the fast-time cellular instability [10], is employed again as the numerical method.

2 Conservation Equations

The readers who wish to find the detailed derivation steps would be referred to the previous paper by Kim et al. [8].

2.1 The Structure equation for the mean field

The mean-field inner structure is described by the famous Liñán's canonical equation for the diffusion flame regime [3]

$$\Theta_{\xi\xi} = \Delta(\Theta - \xi)(\Theta + \xi) \exp\{-(\Theta + \gamma\xi)\}, \quad (1)$$

$$\Theta_{\xi} \rightarrow \pm 1 \quad \text{as} \quad \xi \rightarrow \pm\infty,$$

$$\Theta_F = \Theta - \xi, \quad \Theta_O = \Theta + \xi. \quad (2)$$

where $(\Theta, \Theta_F, \Theta_O)$ is the inner (temperature, fuel, oxidizer) variable, ξ is the stretched inner coordinate and Δ is the reduced Damköhler number of order unity. The factor γ measures the degree of asymmetry in the thermal diffusion across the reaction zone. For positive (negative) γ , the heat loss to the oxidizer (fuel) side is greater and the fuel (oxidizer) leakage is greater. We only need to solve for $0 \leq \gamma < 1$ because of the symmetry in γ . In this analysis, our numerical calculation is limited to the case of $\gamma = 0$.

The mean-field solution could be better represented by the fuel leakage $\alpha = \Theta_F(\xi \rightarrow \infty)$. From the typical variation of α with Δ , it can be found that there exists a minimum value of Δ , below which no solution exists. The condition of minimum Δ is a saddle-node bifurcation point (or turning point), in the vicinity of which interesting dynamic behaviors are to be found.

Since the instability spectrum needs to be parameterized by a reaction-state variable, the logarithmic derivative $\Delta' \equiv \Delta^{-1} d\Delta/d\alpha$ is chosen to represent the state of reaction, where Δ' is a single valued function of the degree of nonequilibrium throughout the entire solution branch of Eq. (1). For $\alpha \rightarrow 0$,

$\Delta' \rightarrow -\infty$. With increasing α , Δ' gradually increases and eventually reaches the turning point (i.e. the condition of minimum Δ) with $\Delta' = 0$, beyond which Δ' becomes positive and keeps increasing. Since $\Delta' = 0$ at the turning point, it is quite convenient to identify the approximate location of the reaction state from the sign of Δ' .

2.2 The Conservation equations for the linear stability analysis

With the simplification of the Lewis numbers identical for the both fuel and oxidizer, the differential equations describing the time-dependent behavior of an infinitesimally small normal-mode perturbation are written as

$$\begin{aligned} \psi_{\xi\xi} - (S + K^2)\psi &= \chi_{\xi\xi} - (LS + K^2)\chi \\ &= \Delta \exp\{-(\Theta + \chi\xi)\} [2\Theta\chi - (\Theta^2 - \xi^2)\psi], \end{aligned} \quad (3)$$

where (ψ, χ) is the eigenfunction for the inner-zone (temperature variable, fuel (or oxidizer)) variable. The boundary conditions to Eq. (3) are $(\psi, \chi) \rightarrow 0$ as $\xi \rightarrow \pm\infty$, from matching with the outer region, where the perturbations are found to be vanishing at the leading order since the perturbations are too fast and too short for them to survive in the outer layer. It is often impractical to impose the strong boundary condition because it requires too big a calculation domain for the eigensolution to converge. Therefore, we rather employ a weaker boundary condition given as

$$(\psi_\xi, \chi_\xi)_{\pm\infty} \rightarrow \mp \sqrt{(1, L)S + K^2} (\psi, \chi)_{\pm\infty}. \quad (4)$$

In this stability problem, L and Δ' , are the control parameters. The problem is then posed as that of finding the eigenvalue S as a function of the wave number K for specified values of the Lewis number L and Δ' .

2.3 Numerical method

Prior to the analysis of the linear stability problem, we solve the mean-field inner-zone problem numerically by using the shooting and relaxation methods. Here we skip the description of numerical scheme since it was already explained in detail in our previous paper [10].

Once the mean-field solution is obtained, we solve for the linear stability problem numerically by using the Evans function method [11]. Employing this approach, the spectral problem in Eqs. (3) and (4) can be reduced to the search of zeroes of the Evans function $D(S)$, which has an important property : $D(S) = 0$ for some given value of S if and only if, for this value of S , Eq. (3) has at least one solution bounded for both $\xi \rightarrow \pm\infty$ and satisfying the boundary conditions in Eq. (4). Consequently, we can look for zeroes of the Evans function, instead of solving linear stability problem in Eqs. (3) and (4) directly.

3 Instability Characteristics with $K = 0$

In this section we discuss the stability of the mean-field solution with respect to planar (or one-dimensional) perturbations, i.e. perturbations with $K = 0$, which will serve as a guideline for the more general two-dimensional stability analysis. The dependence of $S(K = 0)$ on Δ' for various values of L is first considered. The numerical results for ReS vs K^2 , shown in Fig. 1, reveal that there can be two different types of qualitative behavior across a critical value of the Lewis number, denoted by L_c , where L_c is found to be $L_c = 1.4458$.

As shown in Fig. 1a, the primary eigenvalue S for $L = 1.4 < L_c$ is purely real and monotonically increasing with Δ' . As Δ' de-

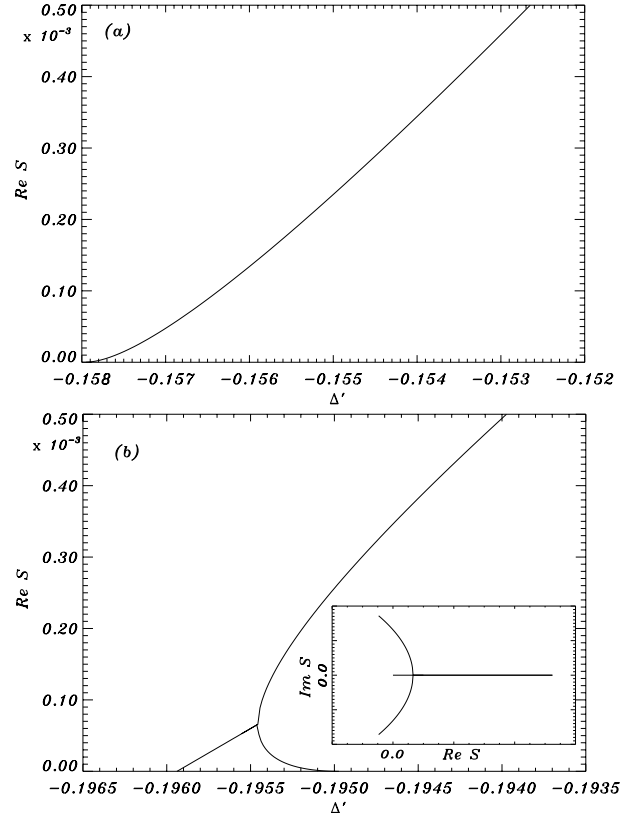


Figure 1: Dependence of ReS on Δ' for $K = 0$: (a) for $L = 1.4$ and (b) for $L = 1.5$.

creases, i.e. decreasing reactant leakage, the point of the discrete spectrum moves along the real axis with decreasing S , indicating weaker instability. The decrease of S with decreasing Δ' continues until a critical value $\Delta' \approx -0.158$, where the eigenvalue merges with the origin, below which the spectrum is no longer discrete. In comparison with the instabilities for $L < 1$, the instabilities for $L > 1$ is seen to be much stronger from the fact that the instability emerges at a much smaller value of Δ' . Although the eigenvalue S with $K = 0$ shows a similar characteristics for $L > 1$ and $L < 1$, it does not imply that the instability characters are similar. Perhaps the full dispersion relationship as well as nonlinear stability analysis would be needed to reveal the full instability characters.

As shown in Fig. 1b for $L = 1.5 > L_c$, variation of the eigenvalue S with Δ' is different from that for $L < L_c$. The onset condition for instability now corresponds to $\Delta' = -0.1959$, a value much smaller than $\Delta' = -0.1579$ for $L = 1.4$, thereby indicating a stronger instability. However, the more important difference lies in the fact that the unstable branch, emerging at the onset value of $\Delta'_1 = -0.1959$, is now a branch of complex conjugates. Increasing Δ' from the onset condition, ReS increases monotonically while the conjugate pair approaches to the real axis. Upon reaching the second critical condition at $\Delta' = -0.19545$, the eigenvalue turns into a real double root with $S \approx 6.9 \times 10^{-5}$, from which two separate real roots bifurcate. Then, the greater eigenvalue continues to increase while the smaller eigenvalue approaches the origin. Beyond the third critical $\Delta' = -0.19498$, the secondary real zero remains at the origin, while the primary real zero continues to move along the real axis with increasing magnitude. Here, it is worthy of note that the range between the first and third critical conditions is extremely narrow and a careful attention needs to be paid in order to resolve the region

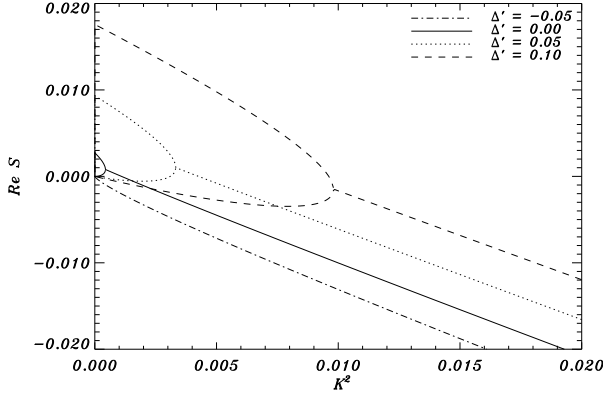


Figure 2: Dispersion relation ReS vs K^2 for $L = 1.1$

exhibiting the non-monotonic behavior.

4 Instability Characteristics for General K

Now we lift the restriction on K in order to consider two-dimensional perturbations. We examine the dispersion relations $S(K)$ for two cases of L , one for $L = 1.1 < L_c$ (shown in Fig. 2) and another one for $L = 1.9 > L_c$ (shown in Fig. 3).

4.1 Dispersion relation for Lewis numbers less than L_c

We first take the case of $L = 1.1 < L_c$. For $\Delta' = 0.0, 0.05$ and 0.1 in Fig. 2, the dispersion relation is seen to possess the both real and complex eigensolution branches. For smaller wave numbers, the primary eigensolution is real, whereas the complex branch bifurcates from the double root of the real branch. This behavior is completely different from that for $L < 1$, where the dispersion relation is real and single-valued for all wave numbers and possesses the maximum growth rate at a finite wave number, therefore exhibiting a cellular instability. However, for $1 < L < L_c$, the real branch persists only up to a finite wave number. In addition, the secondary zero at the origin, i.e. $S(K=0) = 0$, now comes into play by forming a continuous real branch with the primary zero departing from the positive side of the ReS axis. As K^2 increases, the primary and secondary eigenvalues get closer to form a double root, from which a conjugate pair of complex eigensolution bifurcate.

For larger values of Δ' , the instability tends to be strengthened in that the growth rate at any wave number is greater and the extent of real branch also increases. On the other hand, for smaller values of Δ' , the tendency of instability diminishes and the instability disappears if Δ' falls below the onset condition, below which complex eigensolution comes out from the origin at $S(K=0) = 0$ and remains complex with $ReS < 0$ for all wave numbers. Therefore the solution remains stable and the stability boundaries for one- and two-dimensional perturbations are identical. The instability behavior shown in Fig. 2 is often called pulsating instability since the nonlinear instability corresponding to this type of dispersion relation is said to be predominantly uniform in space and oscillatory in time [12].

4.2 Dispersion relation for Lewis numbers greater than L_c

Taking the case of $L = 1.9 > L_c$, the dispersion relation is presented separately in two figures because the transitional characteristics is much more complicated than that for $1 < L < L_c$.

In Fig. 3a, ReS is plotted as functions of K^2 for $\Delta' \leq -0.3691$. For sufficiently small $\Delta' < -0.4093$, the solution is found to

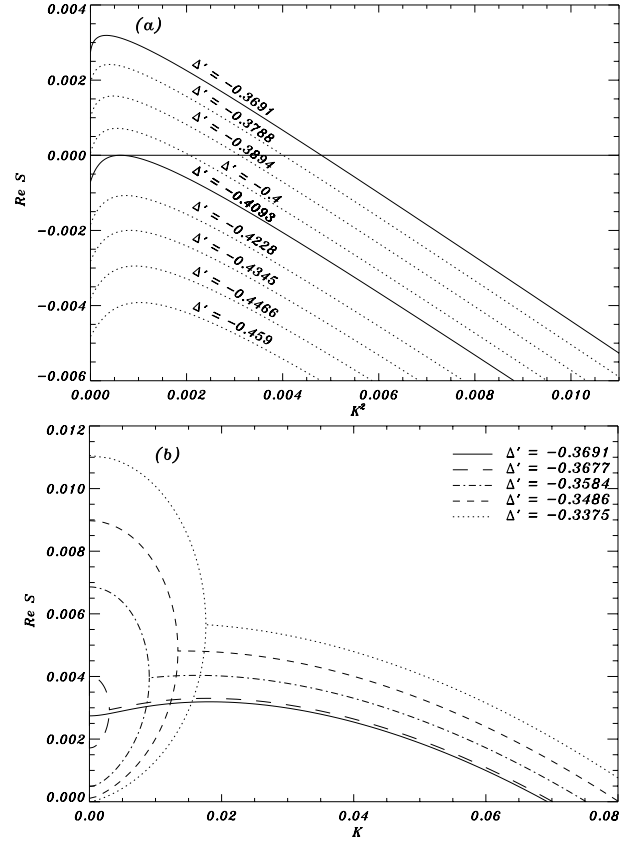


Figure 3: Dispersion relation ReS vs K^2 for $L = 1.9$: (a) for $\Delta' \leq -0.3691$ and (b) for $\Delta' \geq -0.3691$.

be stable since $ReS < 0$ for all values of K . Reaching a critical value of $\Delta' = -0.4093$, the curve of $ReS(K)$ touches the axis of $ReS = 0$ at a finite wave number $K^2 = 0.000625$. If $\Delta' > -0.4093$, there exists an interval of K in which $ReS \geq 0$ and $ImS \neq 0$, exhibiting an instability of traveling nature. Since the traveling instability occurs with a finite wave number, two-dimensional perturbations are more unstable than one-dimensional perturbations. Therefore, unlike the situation encountered for $1 < L < L_c$, the stability boundaries for one- and two-dimensional perturbations are not coincident.

The real part of S vs K for $\Delta' \geq -0.3691$ is shown in of Fig. 3b. Increasing Δ' above the critical value -0.3691 , a real branch with $ReS > 0$ appears in a range of wave number $0 < K < K_c$ whereas the branch for $K > K_c$ remains to be complex. At the critical condition $\Delta' = -0.3691$, a real double root with $ReS > 0$ is first formed at $K = 0$, from which a non-monotonic complex branch with the maximum growth rate occurring at a finite wave number comes out. For Δ' slightly greater than -0.3691 ($\Delta' = -0.3677, -0.3584$ in Fig. 3b), the real eigenvalues at $K = 0$ are splitted and move away from each other while forming a half loop in $0 < K < K_c$ with a conjugate pair of complex eigensolutions coming off from $K = K_c$. The maximum growth rate for the complex branch is still found away from the bifurcation point, but the traveling tendency is much weakened with increasing Δ' . Further increasing Δ' ($\Delta' = -0.3486, -0.3376$ in Fig. 3b), the secondary real eigenvalue become anchored at the origin of $K-ReS$ plane, while the primary real eigenvalue keeps growing. The dispersion relations for $\Delta' = -0.3486, -0.3376$ are very similar to those for $\Delta' = -0.3677, -0.3584$, but the real parts of S for their complex branches are now found to be monotonically decreasing. Far above the transitional region, the

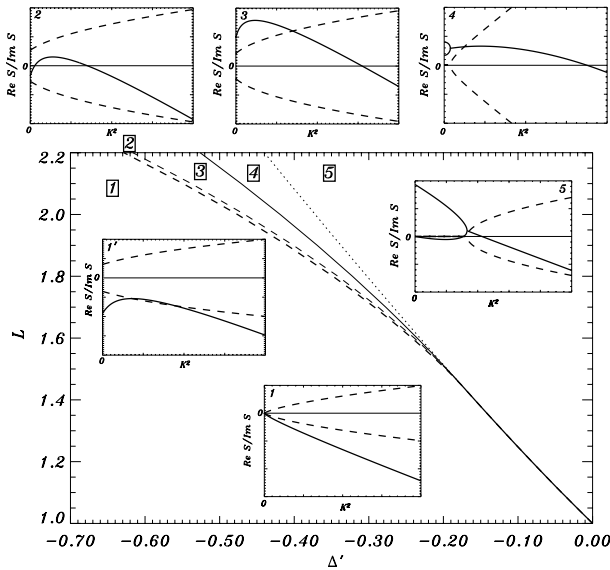


Figure 4: Instability boundaries mapped on the L vs Δ' plane.

overall character is seen to be identical to that of $1 < L < L_c$ shown in Fig. 2.

For $L > L_c$, the overall instability characteristics is found to be traveling and/or pulsating. Near the onset condition, the instability possesses a traveling nature. However, as the value of Δ' becomes larger, pulsating nature is strengthened. Perhaps, in the vicinity of the region where the unstable real branch first emerges, the instability characteristics may demonstrate a traveling instability mixed with pulsating mode.

4.3 Summary of the transitional characteristics

Summarizing the results of the investigation, the instability boundaries, mapped in the L vs Δ' plane, are shown in Fig. 4, in which five regions with different types of dispersion relation can be found in turn from the left to the right. In each region, its typical dispersion relation, in terms of S (vertical axis) vs K^2 (horizontal axis), is shown in the corresponding subfigure, where the solid line represents ReS while the dashed line represents ImS .

As seen from Fig. 4, the boundary for the marginal stability, beginning at $L = 1$, $\Delta' = 0$ and extending to the region of higher L and lower Δ' , is drawn by the two thick lines, i.e. the thick solid line for $1 < L < L_c$ and thick dashed line for $L > L_c$. At the point, located at $L = L_c \approx 1.4458$ and $\Delta' = -0.158$, there exists a switch of bifurcation type between the saddle-node bifurcation (marked by the thick solid line) and the Hopf bifurcation (marked by the thick dashed line). In addition to the boundaries 1-2 and 1-5, the additional boundaries 2-3 (thick dashed line), 3-4 (thin solid line) and 4-5 (thin dotted line) also intersect with each other at the same switch point. This switch point corresponds to the Bogdanov-Takens bifurcation and it is responsible for the switching between different regimes of instability.

5 Conclusions

The fast-time instability of diffusion flames is numerically investigated for Lewis numbers greater than unity by an order unity. Since the scaling employed for the instability analysis is that of the inner reactive-diffusive zone, the analysis became independent of the detailed flow-field structures and the stability character obtained from the present analysis would serve as a generic character to be found in diffusion-flame instabilities.

In contrast to cellular instability for Lewis numbers less than unity, flames with Lewis numbers greater than unity exhibit oscillatory instability. Moreover, the detailed nature of oscillatory instability is found to differ by the degree of deviation of the Lewis number from unity and by the degree of chemical nonequilibrium. First of all, there exists a critical Lewis number at $L_c = 1.4458$, across which the transitional route to instability varies. For Lewis numbers between unity and L_c , the transition to instability occurs in a single stage by a saddle node bifurcation. On the other hand, for Lewis numbers greater than L_c , the transition to instability occurs in a multi-stage manner. First, as entering the unstable parametric domain, the traveling instability is found, so that the onset of instability is associated with the Hopf bifurcation. As further moving into the unstable domain, a small half-loop-shaped real branch emerges from $K = 0$ and eventually dominating the overall instability character. Therefore, the instability character is initially traveling but becomes uniform oscillatory as flames become more unstable. The switch of the bifurcation characters at $L = L_c$ is identified as the Bogdanov-Takens bifurcation.

6 Acknowledgements

The first author would like to thank the Korea Institute of Science and Technology for providing the financial support through the Creative Research Initiative Grant No. 2E18380.

7 References

- [1] Buckmaster, J. D., Nachman, A. and Taliaferro, S., The fast time instability of diffusion flames, *Physica*, **9D**, 1983, 408.
- [2] Peters, N., On the stability of Liñán's "premixed flame regime", *Combust. Flame*, **33**, 1978, 315.
- [3] Liñán, A., The asymptotic structure of counterflow diffusion flame for large activation energies, *Acta Astronautica*, **1**, 1974, 1007.
- [4] Pereira, C. A. and Vega, J. M., Global stability of a premixed reaction zone (time-dependent Liñán's problem), *SIAM J. Math. Anal.*, **21**, 1990, 884.
- [5] Stewart, D. S. and Buckmaster, J. D., The stability of Liñán's 'premixed flame regime' revisited, *SIAM J. Appl. Math.*, **46**, 1986, 582.
- [6] Lozinski, D. and Buckmaster, J. D., "The fast-time stability of a simple deflagration," *Combust. Sci. Technol.*, **111**, 1995, 379.
- [7] Kim, J. S., On the onset condition of fast-time instability in Liñán's premixed-flame regime, *Combustion Theory and Modelling*, **2**, 1988, 273.
- [8] Kim, J. S., Williams, F. A. and Ronney, P. D., Diffusional-thermal instability of diffusion flames, *Journal Fluid Mech.*, **327**, 1996, 273.
- [9] Turing, A. M., The chemical basis of morphogenesis, *Phil. Trans. Roy. Soc. London*, **B237**, 1952, 37.
- [10] Kim, J. S. and Gubernov, V. V., "On the fast-time cellular instabilities of Liñán's diffusion flame regime," To Appear in *Combust. Sci. Technol.*, 2005.
- [11] Evans, J. W., "Nerve axon equations: III Stability of the nerve impulses," *Indiana Univ. Math. J.*, **22**, 1972, 577.
- [12] Cross, M. C. and Hohenberg, P. C., Pattern formation outside of equilibrium, *Review of Modern Physics*, **65**, 1993, 854.